

Observations of heteroclinic bifurcations in resistive magnetohydrodynamic simulations of the plasma response to resonant magnetic perturbations

T. E. Evans ^{1,*} W. Wu,¹ G. P. Canal,² and N. M. Ferraro ^{3,†}

¹General Atomics, P.O. Box 85608, San Diego, California 92186-5608, USA

²Department of Applied Physics, Sao Paulo University, Sao Paulo, CEP 05508-090, Brazil

³Princeton Plasma Physics Laboratory, PO Box 451, Princeton, New Jersey 08543-0451, USA



(Received 14 July 2020; accepted 5 November 2020; published 19 January 2021)

A class of topological magnetic island bifurcations that has not previously been observed in toroidal plasmas is described. Increasing an externally applied three-dimensional magnetic field in resistive magnetohydrodynamic simulations results in the asymmetric elongation of resonant island flux surfaces followed by a sequence of heteroclinic bifurcations. These bifurcations produce new sets of hyperbolic-elliptic fixed points as predicted by the Poincaré-Birkhoff fixed point theorem. Field line calculations verify that the new fixed points do not connect to those of the prebifurcated islands as required for heteroclinic bifurcations on a torus with winding numbers composed of common integer factors.

DOI: [10.1103/PhysRevE.103.013209](https://doi.org/10.1103/PhysRevE.103.013209)

I. INTRODUCTION

Resistive magnetohydrodynamic (MHD) theory and numerical simulations are fundamental tools for studying the physics of magnetic field line tearing and reconnection [1] in astrophysical [2], solar [3], space [4] and magnetically confined toroidal plasmas [5]. Path integrals, tangent to the three-vector magnetic fields from these simulations, are widely used to study the effects of the equilibrium magnetic field line topology on confinement and stability in toroidal plasma devices. Understanding the complexities of the equilibrium topology arising from small external three-dimensional (3D) magnetic field errors and control coil perturbations, as well as the MHD response to these perturbations, is important for the success of fusion energy production. In resonantly perturbed magnetized toroidal plasmas, such as those in tokamaks and stellarators, resistive MHD theory indicates that only three parameters are required to determine the topology of a fully reconnected magnetic state, namely the normalized plasma viscosity, rotation, and resistivity [6]. As discussed in this article, plasma response studies of resonantly perturbed tokamak plasmas with the M3D-C¹ resistive MHD code [7] have resulted in the observation of a class of topological magnetic field line bifurcations, shown in Fig. 1, that does not fit into the existing resistive MHD three-parameter bifurcation theory. Therefore, these results extend forced resonant tearing and reconnection theory to include the creation of new pairs of elliptic and hyperbolic fixed points inside each of the original set of island fixed points, while conserving the winding number of the original island. This process is of particular importance for understanding the physics of self-organization in

toroidal plasmas. Understanding the mechanisms responsible for this class of topological bifurcations is of particular importance as the plasma parameters in high-power toroidal fusion devices approach those needed to achieve self-sustained burning or ignited states, since the ability of the plasma to self-organize can open access to new types of operating regimes.

Experience has shown that, as the magnetic topology changes in tokamaks, unexpected types of plasma dynamics can appear. In particular, bifurcations of the equilibrium magnetic topology are known to be associated with the ability of the plasma to self-organize in unanticipated ways. For example, the spontaneous generation of a bifurcated helical magnetic core and saturated internal kinks, observed in several conventional aspect ratio tokamaks [8,9] and in a small aspect ratio spherical tokamak [10,11], are found to be associated with peaked pressure profiles that trigger bifurcated MHD equilibrium states reminiscent of saturated internal kink modes in ANIMEC simulations [12]. In the RFX-mod reversed field pinch, it is found that as the plasma current is increased, the hyperbolic (x) point of the dominant core magnetic island merges with the main magnetic axis to form a new self-organized, quasi-single-helicity, state [13]. Core magnetic islands have also been found to trigger internal transport barriers [14] and to spontaneously generate cyclical dynamics in the heat transport across low-order rational surfaces near the midradius of the DIII-D tokamak and the large helical device (LHD) [15]. Consequently, understanding the underlying physics responsible for triggering self-organized plasma states is of paramount importance for the development of magnetic fusion energy devices and is of intrinsic interest from a broader scientific perspective.

In magnetically confined toroidal plasmas, such as in tokamaks and stellarators, nonaxisymmetric magnetic field perturbations, from sources external to the plasma along with internal MHD plasma instabilities, produce complex magnetic

*Deceased.

†Corresponding author: nferraro@pppl.gov

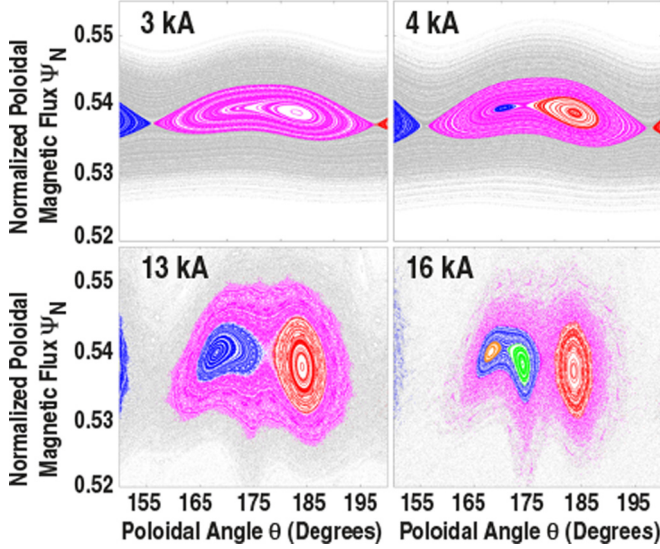


FIG. 1. Topological changes of the inner flux surfaces of $q(\psi_N) = 3$ magnetic islands as the current (I_{NCC}) in a 3D control coil is increased from 3 to 16 kA.

equilibria. As the plasma pressure increases, changes in the equilibrium magnetic topology, plasma stability, and transport become highly sensitive to the external nonaxisymmetric vacuum field perturbations. An important metric for quantifying this effect is the ratio of the volume averaged plasma pressure to the magnetic pressure, $\beta = \langle p \rangle / (B^2 / 2\mu_0)$, when normalized by the product of the minor radius of the plasma (a) and the toroidal magnetic field (B_T) divided by the plasma current (I_p), $\beta_N = \beta(aB_T / I_p)$. Changes in the resonant and nonresonant magnetic equilibrium topology, caused by vacuum field perturbations, in combination with the MHD plasma response, result from either amplification or screening of the external field. These changes are known to alter neoclassical tearing mode (NTM) and edge localized mode (ELM) stability, as well as the particle, energy, and momentum confinement of the plasma [16]. Coupling between stable ideal kink modes and resonant modes on rational surfaces with $m = nq$ have been shown to correlate with reductions in the edge pressure gradient resulting in changes to the ELM stability [17,18]. Here, m and n are poloidal and toroidal mode integers, respectively, and $q(\psi_N)$ is the safety factor associated with the axisymmetric equilibrium magnetic field, where ψ_N is the normalized equilibrium field poloidal flux. Therefore, the coupling between stable ideal kink modes, with m, n components that reside on a resonant $q(\psi_N)$ surface, can significantly modify the resonant MHD plasma response to an external magnetic perturbation field.

II. MODELING AND OBSERVATION OF HETEROCLINIC BIFURCATIONS

In this article, the plasma response to a single $n = 3$ toroidal mode from externally applied nonaxisymmetric magnetic perturbation fields ($\delta \vec{b}^{\text{ext}} = \delta b_r^{\text{ext}} \hat{r} + \delta b_\theta^{\text{ext}} \hat{\theta} + \delta b_\phi^{\text{ext}} \hat{\phi}$) is simulated in two high $-\beta_N$ spherical tokamak discharges using the linear M3D-C¹ resistive MHD code. It is shown that the applied $n = 3$ toroidal mode results in three isolated

sets of $m = 3, n = 1$ magnetic islands on the $q = 3$ surface. We refer to these three isolated sets of islands as heteroclinic islands since the fixed x (hyperbolic) and o (elliptic) points, along with the associated internal flux surfaces of each set, do not connect to the other two sets of islands. The distinction between homoclinic islands, such as $m = 2, n = 1$ islands, where the fixed points and flux surfaces connect to each other, and heteroclinic islands is a fundamental feature of the observed bifurcation process discussed here. The M3D-C¹ simulations result in the formation of three new $m = 3, n = 1$ sets of heteroclinic islands on the $q = 3$ surface, as required to preserve the island winding number $N_w = m/n$, where field lines originating on each fixed point make m toroidal revolutions to complete n poloidal revolutions. It is also found that heteroclinic bifurcation occurs on each of the low-order rational surfaces from the center of the plasma towards the edge as $\delta \vec{b}^{\text{ext}}$ is increased. These are referred to as internal topological bifurcations of the island since resistivity, viscosity, and rotation are kept fixed for all of these simulations. Here, the total resonant magnetic field in the plasma is $\delta \vec{b}^{\text{total}} = \delta \vec{b}^{\text{ext}} + \delta \vec{b}^{\text{plasma}}$, with $\delta \vec{b}^{\text{plasma}}$ being the resistive MHD plasma response field due to the application of $\delta \vec{b}^{\text{ext}}$. It is found that the threshold value of $\delta \vec{b}^{\text{ext}}$ required for the bifurcation depends on β_N .

The linear time-independent single- and two-fluid M3D-C¹ simulations in this work were carried out using synthetically generated kinetic Grad-Shafranov [19] plasma equilibria in the NSTX-U spherical tokamak [20]. Two equilibria were simulated: one with a $\beta_N = 5.5$, $I_p = 1.5$ MA, $B_T = 1.0$ T and a safety factor on the 95% normalized flux surface $q_{95} = 8.7$, and another with $\beta_N = 7.6$, $I_p = 2.0$, $B_T = 1.0$, and $q_{95} = 5.5$. The safety factor on axis (q_0) is 1.25 in both cases. Nonaxisymmetric vacuum field perturbations are applied using 12 equally spaced toroidal rectangular coils above and below the equatorial plane, referred to as the nonaxisymmetric control coils (NCCs). This coil set is being considered for installation in NSTX-U over the next few years. In the simulation discussed here, the normalized currents in this set of coils have a toroidal distribution pattern in the upper NCCs of $(+1, 0, -1, 0, +1, -1, 0, +1, 0, -1, 0, 0)$ with opposite signs in the lower NCCs. M3D-C¹ simulations are done with currents in the NCC (I_{NCC}) ranging from 1 to 30 kA using only the $n = 3$ Fourier component and the radial plasma profiles shown in Fig. 2 as input.

Due to the relatively high poloidal $\vec{E} \times \vec{B}$ rotation in these discharges, shown in Fig. 2(d), the M3D-C¹ simulations show that the resonant component of $\delta \vec{b}^{\text{total}}$ is reduced by at least a factor of 2 due to screening on the resonant surfaces of interest compared to that of $\delta \vec{b}^{\text{ext}}$. This results in small magnetic islands, with widths $\Delta \psi_N^{\text{island}} \leq 0.01$, formed on each rational surface.

In the unperturbed $\delta \vec{b}^{\text{ext}} = 0$ simulations, field lines are confined to the surface of a 3D torus defined by ψ_N , the normalized toroidal flux χ_N , the poloidal angle θ , and the toroidal angle ϕ , where $(\psi_N, \theta, \chi_N, \phi)$ are referred to as action-angle variables. Using this representation, the action ψ_N , when plotted as a function of the poloidal angle θ , describes a set of parallel straight field lines that intersect a 2D Poincaré plane at $\phi = \text{const}$. On rational toroidal surfaces, field lines form

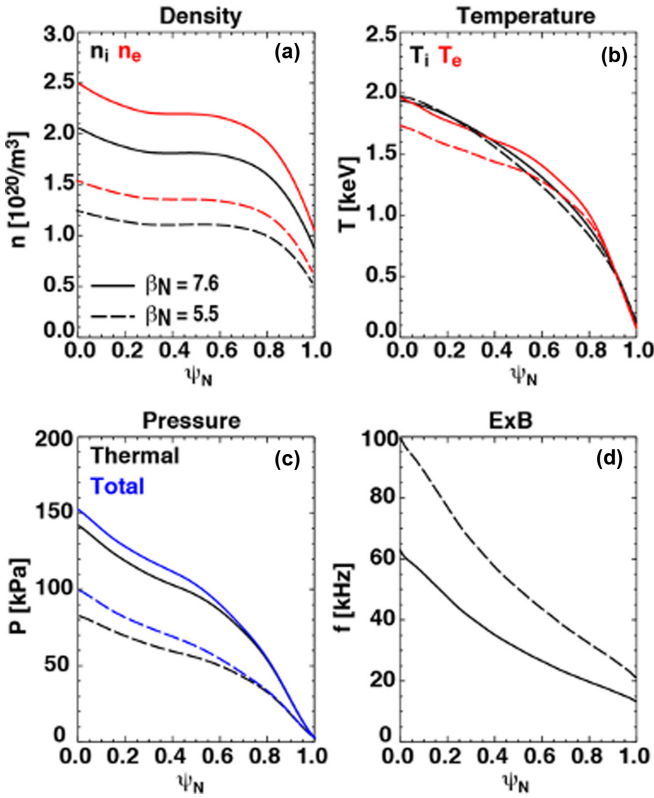


FIG. 2. (a) Ion (black) and electron [red (grey)] density, (b) ion (black) and electron [red (grey)] temperature, (c) thermal (black) and total [blue (grey)] pressure, and (d) poloidal $\vec{E} \times \vec{B}$ rotation ($\omega_{\vec{E} \times \vec{B}}$) for $\beta_N = 7.6$ (solid line) and $\beta_N = 5.5$ (dashed line) cases.

periodic geodesic helical trajectories, which result in a dense set of fixed points when projected on the Poincaré plane. For example, in the unperturbed axisymmetric case, individual $q(\psi_N) = 3$ fixed-point field lines undergo three toroidal revolutions ($\phi = 6\pi$) before returning to their original ψ_N, θ position, as prescribed by the winding number $N_w = m/n$. The application of a small $\delta\vec{b}^{\text{ext}}$ field destroys the toroidal symmetry resulting in the formation of an even multiple of fixed points as a consequence of the Poincaré-Birkhoff fixed-point theorem [21].

According to the Poincaré-Birkhoff fixed-point theorem, an even number of fixed points must appear on every rational surface for an arbitrarily small $\delta\vec{b}^{\text{ext}}$. In conservative area or magnetic flux preserving ($\vec{\nabla} \cdot \vec{B} = 0$) Hamiltonian systems, where each rational surface is bounded on both sides by an irrational surface, the KAM theorem [22], in conjunction with the Poincaré-Birkhoff fixed point theorem, mandates that each pair of fixed points must consist of a hyperbolic and an elliptic point. In general, this allows for the formation of $N_{\text{fp}} = 2\ell m$ fixed points, where m is the period of each fixed point, ℓ is referred to as the topological index corresponding to the number of isolated fixed-point pairs, and 2 is the Poincaré-Birkhoff integer. Since topological island bifurcations must preserve the fixed-point winding number on each resonant surface of the torus, we have $\ell = 1$ for homoclinic islands and $\ell > 1$ for heteroclinic islands. An example of a set of heteroclinic islands resulting from the M3D-C¹ $\beta_N = 5.5$ simulation on the

$q(\psi_N) = 3$ surface in NSTX-U with $I_{\text{NCC}} = 2.0$ kA is shown in Fig. 3. Here, three isolated heteroclinic sets ($\ell = 3$) of period 3 ($m = 3$) islands are formed when the NCC is turned on, each of which is comprised of three elliptic fixed-points (o points) and three hyperbolic fixed points (x points), resulting in $N_{\text{fp}} = 2\ell m = 18$. As shown by colors/shades in Fig. 3, field line trajectories corresponding to one set of heteroclinic islands do not connect to either of the other two heteroclinic island sets.

Figure 1 shows a detailed view of the $q(\psi_N) = 3$ MHD magnetic island with its elliptic fixed point at $\theta = 179.9^\circ$ in Fig. 3 for increasing I_{NCC} levels. With $I_{\text{NCC}} = 3.0$ kA, $\Delta\psi_N^{\text{island}}$ increases slightly compared to the island with $I_{\text{NCC}} = 1.0$ kA and the elliptic fixed point moves from $\theta = 179.9^\circ$ to $\theta = 183.1^\circ$, while a subset of internal island flux surfaces stretches asymmetrically in the opposite direction toward the screened vacuum island elliptic point located at $\theta = 163.3^\circ$. This asymmetric flux surface stretching is consistent with a change in $\delta\vec{b}^{\text{plasma}}$ when linearly superimposed on the $\delta\vec{b}^{\text{ext}}$ field, and is expected to involve a redistribution of the screening current. With $I_{\text{NCC}} = 4.0$ kA, the elongated lobe has bifurcated to form three new sets of elliptic and hyperbolic fixed points. We refer to this as a *topological heteroclinic island bifurcation*, where $\ell_b = 2\ell = 6$ resulting in $N_{\text{fp}} = 2\ell_b m = 36$, as required to preserve the $m/n = 3/1$ winding number in each set of islands. The bifurcation occurs at $I_{\text{NCC}} = 3.48$ kA in this case.

As I_{NCC} continues to increase beyond 3.48 kA, the original MHD island elliptic fixed point moves to $\theta = 184.5^\circ$ while the new elliptic fixed point moves to $\theta = 168.2^\circ$ and the new hyperbolic fixed point moves to $\theta = 175.7^\circ$. These fixed points continue to move poloidally by small amounts as I_{NCC} is increased to 14.7 kA where a second heteroclinic bifurcation takes place. This second bifurcation results in three new heteroclinic sets of isolated $m = 3$ islands, with $\ell_{2b} = 1.5\ell_b = 9$ resulting in $N_{\text{fp}} = 2\ell_{2b} m = 54$. These heteroclinic bifurcations also occurs on each of the period 3 rational surfaces studied in this simulation starting at $q(\psi_N) = 6/3$ and cascading radially outward, down the pressure profile shown in Fig. 2(c), as I_{NCC} is increased. A similar process is observed during simulations of the $\beta_N = 7.6$ case but, in this case, only one bifurcation occurs on the $q(\psi_N) = 3$ surface when I_{NCC} passes through 4.23 kA as it is increased to 30 kA. In general, it is found that forward and reversed heteroclinic bifurcations must satisfy $N_w = m/n$ on the torus when m, n are composed of a common factor. For example, $m, n = 2, 1$ islands bifurcate into two sets of $m, n = 2, 1$ heteroclinic islands as opposed to $m, n = 4, 2$ islands.

Although not visible in the 3.0-kA panels of Fig. 1, due to the generation of a screening current by the MHD plasma response, a vacuum prebifurcated heteroclinic island due to $\delta\vec{b}^{\text{ext}}$ is located inside the MHD island with its elliptic and hyperbolic fixed points on the $q(\psi_N) = 3$ surface at $\theta = 163.3^\circ$ and $\theta = 183.5^\circ$ respectively. Here, the hyperbolic fixed point of the prebifurcated vacuum island is located at approximately the same position as the original elliptic point of the MHD island shown in Fig. 1 with $I_{\text{NCC}} = 3$ kA. Our hypothesis is that the positions of the vacuum island fixed points along with all the nonresonant kink aligned eigenmodes on the $q(\psi_N) = 3$ surface drive the bifurcation dynamics of the MHD islands, as the NCC current is increased, by (1) regulating

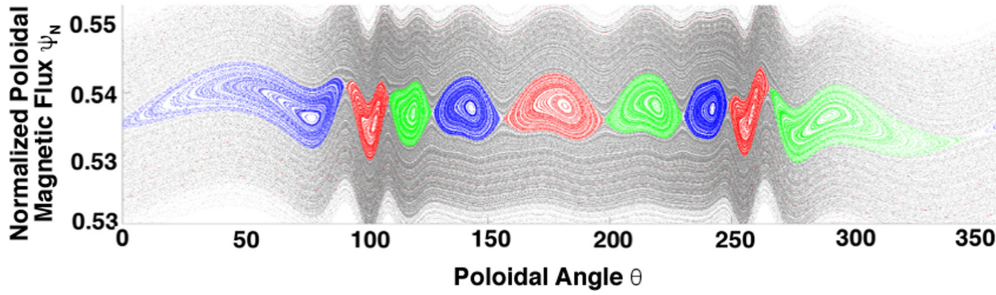


FIG. 3. Three isolated sets of $m/n = 3/1$ heteroclinic magnetic islands, represented by different colors or shades, located on the $q = 3$ normalized poloidal flux surface in NSTX-U during the application of a 2-kA $n = 3$ NCC perturbation field.

the screening current needed to prevent the vacuum island from opening and (2) distorting/stretching the flux surfaces. It is also found that two-fluid M3D-C¹ simulations, with the same plasma parameters as those used during the single-fluid simulations, produce quantitatively equivalent results indicating that the ion dynamics in M3D-C¹ are not playing a role in these heteroclinic bifurcation sequences. Interestingly, linear and nonlinear simulations of rotating $m, n = 2, 1$ tearing mode bifurcations, referred to as flip instabilities, which appear to involve fast transient heteroclinic bifurcations, have found that nonlinear effects, due to inertia in the momentum equation, do not play a role in the bifurcation process [23].

The shift between the topological vacuum island and the MHD island elliptic fixed points in Fig. 1 is expected to result from a redistribution of the plasma current density inside the MHD islands, as seen in gyrokinetic simulations [24]. This is required to maintain the co- I_p vacuum island screening current density filament ($j_{\parallel-\text{vac}}$) while generating a counter- I_p current density filament ($-j_{\parallel-\text{MHD}}$) needed to open the topological island elliptic points. As I_{NCC} increases, $j_{\parallel-\text{vac}}$ is expected to increase in order to maintain a screening current consistent with $\omega_{\vec{e}} \times \vec{B}$ inside each island. A secondary, counter- I_p , $-j_{\parallel-\text{MHD}}$ filament located in the elongated flux surfaces between the screened topological vacuum island and the original MHD island elliptic fixed points is formed as I_{NCC} increases. Eventually, $\delta\vec{b}^{\text{plasma}}$ due to the secondary $-j_{\parallel-\text{MHD}}$ filament cancels $\delta\vec{b}^{\text{plasma}}$ from the original $-j_{\parallel-\text{MHD}}$ filament, and a new set of hyperbolic fixed points with their associated Poincaré-Birkhoff elliptic fixed points are formed.

Recent experiments in DIII-D have shown spontaneous bifurcations from two sets rotating $m, n = 2, 1$ heteroclinic tearing modes to a single rotating $m, n = 2, 1$ homoclinic tearing mode, which verify the $N_w = m/n$ constraint imposed on heteroclinic to homoclinic bifurcations [25].

In addition to satisfying the Poincaré-Birkhoff fixed-point theorem, M3D-C¹ simulations demonstrate that the dynamics of these heteroclinic island bifurcations are the manifestation of a smooth/continuous, invertible, process controlled by $\delta\vec{b}^{\text{ext}}$ that does not result in bistable or hysteresis-like behavior associated with various types of tearing modes [26]. This behavior is consistent with degenerate equilibrium points associated with local saddle-node bifurcations that are found in Hamiltonian systems composed of conservative vector fields [27]. In addition, the process involved in the stretching of the

internal MHD island flux surfaces, leading up to these heteroclinic bifurcations, is consistent with diffeomorphisms found in a conservative dynamical system where subsets of differentiable manifolds undergo smooth one-to-one, invertible, topological transformations as a control parameter is varied. These facts support our conclusion that the observed heteroclinic bifurcations result in the creation of topological islands driven by the penetration of the applied nonaxisymmetric field as opposed to an MHD tearing and reconnection response.

III. SUMMARY

A class of topological heteroclinic bifurcations is described in toroidal plasmas during variations of an externally applied nonaxisymmetric perturbation field in linear single- and two-fluid M3D-C¹ resistive MHD simulations. These bifurcations preserve the rational flux surface winding numbers by generating new sets of isolated, heteroclinic, magnetic islands inside existing heteroclinic MHD magnetic islands starting on rational surfaces near the center of the plasma and cascading outward as the $\delta\vec{b}^{\text{ext}}$ perturbation field is increased. Simulations with different normalized plasma pressures (β_N) result in similar bifurcation sequences but with different values of the $\delta\vec{b}^{\text{ext}}$ bifurcation parameter. As β_N is increased, bifurcations occur at larger $\delta\vec{b}^{\text{ext}}$ values. These bifurcations have been shown to reduce collisional cross-field transport due to the generation of strong internal island stochasticity in the vicinity of the heteroclinic hyperbolic (x) points [28] and have resulted in the observation of different types of self-organized behaviors than those that have been considered previously in toroidal plasmas [25].

ACKNOWLEDGMENTS

This material is based upon work supported by the US Department of Energy Office of Fusion Energy Sciences, using the DIII-D National Fusion Facility, a DOE Office of Science user facility, under Awards No. DE-FC02-04ER54698, No. DE-SC0012706, No. DE-SC0018030, No. DE-SC0020298, No. DE-SC0019078, and No. DE-AC02-09CH11466. This study was also financed in part by the Coordenação de Aperfeiçoamento de Pessoal de Nível Superior-Brasil (CAPES)-Finance Code 001. This report was prepared as an account of work sponsored by an agency of the United States

Government. Neither the United States Government nor any agency thereof, nor any of their employees, makes any warranty, express or implied, or assumes any legal liability or responsibility for the accuracy, completeness, or usefulness of any information, apparatus, product, or process disclosed, or represents that its use would not infringe privately owned rights. Reference herein to any specific commercial product,

process, or service by trade name, trademark, manufacturer, or otherwise does not necessarily constitute or imply its endorsement, recommendation, or favoring by the United States Government or any agency thereof. The views and opinions of authors expressed herein do not necessarily state or reflect those of the United States Government or any agency thereof.

-
- [1] W. D. Gonzalez, E. N. Parker, F. S. Mozer, V. M. Vasyliunas, P. L. Pritchett, H. Karimabadi, P. A. Cassak, J. D. Scudder, M. Yamada, R. M. Kulsrud, and D. Koga, Fundamental concepts associated with magnetic reconnection, in *Magnetic Reconnection Concepts and Application, Astrophysics and Space Science Library* No. 427, edited by W. Gonzalez and E. Parker (Springer International, Switzerland, 2016).
- [2] A. Brandenburg and K. Subramanian, Astrophysical magnetic fields and nonlinear dynamo theory, *Phys. Rep.* **417**, 1 (2005).
- [3] J. C. Santos and J. Büchner, MHD simulations of electric currents in the solar atmosphere caused by photospheric plasma motion, *Astrophys. Space Sci. Trans.* **3**, 29 (2007).
- [4] R. A. Treumann and W. Baumjohann, Collisionless magnetic reconnection in space plasmas, *Front. Phys.* **1**, 31 (2013).
- [5] N. M. Ferraro, Calculations of two-fluid linear response to non-axisymmetric fields in tokamaks, *Phys. Plasmas* **19**, 056105 (2012).
- [6] R. Fitzpatrick, Bifurcated states of a rotating tokamak plasma in the presence of a static error-field, *Phys. Plasmas* **5**, 3325 (1998).
- [7] N. M. Ferraro, T. E. Evans, L. L. Lao, R. A. Moyer, R. Nazikian, D. M. Orlov, M. W. Shafer, E. A. Unterberg, M. R. Wade, and A. Wingen, Role of plasma response in displacements of the tokamak edge due to applied non-axisymmetric fields, *Nucl. Fusion* **53**, 073042 (2013).
- [8] A. Weller, A. D. Cheetham, A. W. Edwards, R. D. Gill, A. Gondhalekar, R. S. Granetz, J. Snipes, and J. A. Wesson, Persistent Density Perturbations at Rational- q Surfaces following Pellet Injection in the Joint European Torus, *Phys. Rev. Lett.* **59**, 2303 (1987).
- [9] A.-L. Pecquet, P. Cristofani, M. Mattioli, X. Garbet, L. Laurent, A. Geraud, C. Gil, E. Joffrin, and R. Sabot, Snake-like phenomena in tore supra following pellet injection, *Nucl. Fusion* **37**, 451 (1997).
- [10] I. T. Chapman, M.-D. Hua, S. D. Pinches, R. J. Akers, A. R. Field, J. P. Graves, R. J. Hastie, and C. A. Michael, and the MAST Team, Saturated ideal modes in advanced tokamak regimes in MAST, *Nucl. Fusion* **50**, 045007 (2010).
- [11] J. E. Menard, R. E. Bell, E. D. Fredrickson, D. A. Gates, S. M. Kaye, B. P. LeBlanc, R. Maingi, S. S. Medley, W. Park, S. A. Sabbagh, A. Sontag, D. Stutman, K. Tritz, and W. Zhu, and the NSTX Research Team, Internal kink mode dynamics in high- β NSTX plasmas, *Nucl. Fusion* **45**, 539 (2005).
- [12] W. A. Cooper, I. T. Chapman, O. Schmitz, A. D. Turnbull, B. J. Tobais, E. A. Lazarus, F. Turco, M. J. Lanctot, T. E. Evans, J. P. Graves, D. Brunetti, D. Pfefferlé, H. Reimerded, O. Sauter, F. D. Halpren, T. M. Tran, S. Coda, B. P. Duval, B. Labit, A. Pochelon *et al.*, Bifurcated helical core equilibrium states in tokamaks, *Nucl. Fusion* **53**, 073021 (2013).
- [13] R. Lorenzini, E. Martines, P. Piovesan, D. Terranova, P. Zanca, A. Alfier, D. Bonfiglio, F. Bonomo, A. Canton, L. Carraro, R. Cavazzana, D. F. Escande, A. Fassian, P. Franz, M. Gobbin, P. Innocente, L. Marrelli, R. Pasqualotto, M. E. Puiatti, M. Spolaore *et al.*, and RFX-mod team and collaborators, Self-organized helical equilibria as a new paradigm for ohmically heated fusion plasmas, *Nat. Phys.* **5**, 570 (2009).
- [14] S. Inagaki, N. Tamura, K. Ida, S. Kubo, T. Shimozuma, Y. Nagayama, K. Kawahata, S. Sudo, A. Fujisawa, K. Itoh, S.-I. Itoh, and LHD Experimental Group, Internal transport barrier formation induced by edge perturbation on LHD, *Nucl. Fusion* **50**, 064012 (2010).
- [15] K. Ida, T. Kobayashi, M. Yoshinuma, Y. Suzuki, Y. Narushima, T. E. Evans, S. Ohdachi, H. Tsuchiya, S. Inagaki, and K. Itoh, Bifurcation physics of magnetic islands and stochasticity explored by heat pulse propagation studies in toroidal plasmas, *Nucl. Fusion* **56**, 092001 (2016).
- [16] T. E. Evans, Resonant magnetic perturbations of edge-plasmas in toroidal confinement devices, *Plasma Phys. Control. Fusion* **57**, 123001 (2015).
- [17] C. Paz-Soldan, N. C. Logan, S. R. Haskey, R. Nazikian, E. J. Strait, X. Chen, N. M. Ferraro, J. D. King, B. C. Lyons, and J.-K. Park, Equilibrium drives of the low and high field side $n = 2$ plasma response and impact on global confinement, *Nucl. Fusion* **56**, 056001 (2016).
- [18] T. E. Evans, R. A. Moyer, K. H. Burrell, M. E. Fenstermacher, I. Joseph, A. W. Leonard, T. H. Osborne, G. D. Porter, M. J. Schaffer, P. B. Snyder, P. R. Thomas, W. P. West, and J. G. Watkins, Edge stability and transport control with resonant magnetic perturbations in collisionless tokamak plasmas, *Nat. Phys.* **2**, 419 (2006).
- [19] L. L. Lao, H. E. S. John, Q. Peng, J. R. Ferron, E. J. Strait, T. S. Taylor, W. H. Meyer, C. Zhang, and K. I. You, MHD equilibrium reconstruction in the DIII-D Tokamak, *Fusion Sci. Technol.* **48**, 968 (2005).
- [20] J. E. Menard, J. P. Allain, D. J. Battaglia *et al.*, Overview of the NSTX Upgrade initial results and modeling highlights, *Nucl. Fusion* **57**, 102006 (2017).
- [21] G. D. Birkhoff, *Dynamical Systems* (Am. Math. Soc. Colloquium Publications, New York, 1927), Vol. IX.
- [22] J. Moser, *Stable and Random Motion in Dynamical Systems* (Princeton University Press, Princeton, 1973).
- [23] P. Maget, O. Février, H. Lürjens, J.-F. Luciani, and X. Garbet, Bifurcation of magnetic island saturation controlled by plasmas viscosity, *Plasma Phys. Control. Fusion* **58**, 055003 (2016).
- [24] G. Domg and Z. Lin, Effects of magnetic islands on bootstrap current in toroidal plasmas, *Nucl. Fusion* **57**, 036009 (2017).

- [25] L. Bardóczy and T. E. Evans, Discovery of magnetic island heteroclinic bifurcation in tokamaks, 62nd Annual Meeting of the APS Division of Plasma Physics, Abstract PO06.00010, Held remotely Nov. 11, 2020.
- [26] P. A. Cassak, M. A. Shay, and J. F. Drake, A saddle-node bifurcation model of magnetic reconnection onset, [Phys. Plasmas](#) **17**, 062105 (2010).
- [27] J. Guckenheimer and P. Holmes, in *Nonlinear Oscillations, Dynamical Systems, and Bifurcations of Vector Fields*, 7th ed. (Springer-Verlag, New York, 2002), pp. 1–459.
- [28] W. Wu, T. E. Evans, G. P. Canal, N. M. Ferraro, B. C. Lyons, and D. M. Orlov, Topological bifurcations of magnetic islands in NSTX-U, [Nucl. Fusion](#) **59**, 066010 (2019).